NUMERICAL SIMULATION OF THE FLOW PAST A MOVING CYLINDER USING AN IMMERSED BOUNDARY METHOD

Débora Gleice da Silva Del Rio Vieira, deboragleicedelrio@gmail.com
Augusto Salomão Bornschlegell, augusto.s.b@gmail.com
Sérgio Said Mansur, mansur@dem.feis.unesp.br
UNESP Ilha Solteira, Av. Brasil Centro, 56, Ilha Solteira – SP, Brazil

Julio Militzer, julio.militzer@dal.ca
Dalhousie University, 1360 Barrington St, Halifax-NS, Canada

Abstract. *Immersed boundary methods have been used as powerful tools for numeric simulation of flow around complex and moving geometries. Even though the immersed method idea is not difficult to understand, its numerical implementation is not simple. Furthermore, numerical results are significantly influenced by different aspects related to the Navier-Stokes equation solver, such as precision order for the time scheme and the advective terms treatment scheme. In the present work, an immersed boundary method based on the virtual physical model has been implemented in an in-house 2D computational code. A numerical study of the flow past an oscillating cylinder placed in an infinite medium has been performed. The influence exerted by several parameters on the results have been investigated; such as the size of the Eulerian and Lagrangian meshes, size of the computational domain and the different ways adopted to impose movement onto the boundaries. The results are compared with data found in the literature and indicate that low precision order of the numerical time scheme can be responsible for the huge sensitivity of the code.*

Keywords*: Immersed Boundary Method, Virtual Physical Model, Moving cylinder.*

1. INTRODUCTION

Most of flow systems typically founded in engineering or biological applications involve complex geometries with moving boundaries. These cause severe difficulties in finding accurate results by means of the numerical solution of the Navier-Stokes equations. Accurate solutions need a correct representation of the physical problem and, consequently, it is necessary to choose a numerical model able to deal with the complexity existing in the real situation.

Different numerical methodologies have been proposed in the last decades to treat this class of problems. In this context, the Immersed Boundary Method, conceived by Peskin (1977), is particularly suited to represent fluid motion inside geometrically arbitrary systems. In brief, Peskin's methodology allows the representation of a body immersed in a passing flow by adding a forcing term to the Navier-Stokes equations. Due to this term, a simple Cartesian mesh could be used even for moving boundaries, just by evaluating the force properly.

The first model developed by Peskin had the focus on the flow passing through a cardiac valve. Since then, several other researchers have improved the original model, changing in essence the way the forcing term is evaluated. According to Mittal and Iaccarino (2005), the different variants of the immersed boundary method can be classified in two major categories: the discrete forcing methods and the continuous forcing methods. In the first one, the force is calculated after the domain discretization, and added to the cells that compose the boundary between the body and the flow. To achieve a better definition of the geometry these methods may need some modifications in the mesh patters around the body but that implies an increase in the computational costs. As examples one can see the model of Verzicco *et al*. (2000) for turbulent flow inside an engine, two-dimensional flows as showed in Balaras (2004), and many others. In the other hand, the continuous forcing approach, evaluates the force before the domain discretization, using a certain function to distribute the force effects through the neighboring cells. These methods have the advantage of using the same mesh without any modifications of the boundaries. They have been used by several researchers like in Fauci and McDonald (1994) to simulate the locomotion of aquatic animals, and by Unverdi and Tryggvason (1992) for bubble dynamics and many others.

By means of the Physical Virtual Model, initially proposed by Lima e Silva (2002), the force calculation is based on the physical interaction between the body and the flow. It is based in the application of the momentum conservation equations in the fluid volumes centered on the Lagrangian points interface components. In this manner the non-slip condition is imposed directly at the interface. For these reasons, the Physical Virtual Model is a very attractive numerical approach, using only one simple Eulerian mesh during the whole simulation, while the body is represented by Lagrangian points. These points do not need to conform to the mesh, which allows the representation of any moving and complex geometry. Basically, a force is added to the Navier-Stokes equations, in the specific location of the Lagrangian points, and distributed to the neighboring cells, as explained in the following section.

In the present work, the flow past a moving cylinder is simulated using the Physic Virtual Model. As a moving geometry, the Immersed Boundary Method selected seems to be adequate for this case, incurring a relatively low computational cost.

2. MATHEMATICAL FORMULATION

The incompressible isothermal flow of a Newtonian fluid is governed by mass conservation and Navier-Stokes equations. For a Cartesian 2D domain, these equations can be written as:

$$\frac{\partial u_m}{\partial x_m} = 0 \tag{1}$$

$$\rho\left[\frac{\partial u_m}{\partial t} + \frac{\partial u_m u_n}{\partial x_n}\right] = \frac{\partial p}{\partial x_m} + \frac{\partial}{\partial x_n}\left[\mu\left(\frac{\partial u_m}{\partial x_n} + \frac{\partial u_n}{\partial x_m}\right)\right] \tag{2}$$

where ρ is the fluid density, μ the kinematic viscosity, p the pressure, u_m and u_n are the velocity vector components.

To represent the immersed body numerically in the flow, one can add a forcing term to the Navier-Stokes equations given by F_m.

$$\rho\left[\frac{\partial u_m}{\partial t} + \frac{\partial u_m u_n}{\partial x_n}\right] = \frac{\partial p}{\partial x_m} + \frac{\partial}{\partial x_n}\left[\mu\left(\frac{\partial u_m}{\partial x_n} + \frac{\partial u_n}{\partial x_m}\right)\right] + F_m \tag{3}$$

When properly evaluated, the forcing term causes the flow to go around moving or complex interfaces represented by the Lagrangian mesh, without the need to impose any local boundary condition.

According to Lima e Silva (2002), the Physical Virtual Model represents this force as a combination of an acceleration force, an inertial force, a pressure force and a viscous force. Respectively:

$$F\left(X_k,t\right) = F_a\left(X_k,t\right) + F_i\left(X_k,t\right) + F_p\left(X_k,t\right) + F_d\left(X_k,t\right) \tag{4}$$

$$F_a = \rho\frac{\partial u}{\partial t} \tag{5}$$

$$F_i\left(X_k,t\right) = \rho\left(u.\nabla u\right) \tag{6}$$

$$F_p\left(X_k,t\right) = \nabla p \tag{7}$$

$$F_d\left(X_k,t\right) = -\nabla.\left(2\mu d\right) \tag{8}$$

where X_k are the Lagrangian points locations, evaluated at the right location of the Lagrangian points, by interpolation of the velocity and pressure fields.

3. THE COMPUTATIONAL PROGRAM

An in-house program was used as a base code for implementing the immersed boundary method desired in the present work. The code is a 2D solver for the Navier-Stokes equations in Cartesian coordinates by Finite Volume developed by Campregher (2002). The user can chose between SIMPLE and SIMPLEC for the velocity couple, and Upwind, Second Order Upwind, Central Difference, Power Law and Quick, for advective terms treatment. Also for turbulent flows, there were chosen the LES and Smagorinsky subgrid model. The code was written in FORTRAN 95 organized and prepared to receive new routines for implementing different methods in the base code. Bornschlegell (2008) added new modules to make possible the use of the Virtual Physical Model (Lima e Silva, 2002) in the Immersed Boundary Method.

For simulating the cylinder in the present work, let consider it formed with points where a force will be added.

These points are the Lagrangian mesh and it is immersed in another mesh, a Cartesian and regular one, as shown in Fig. 1. So, for the domain, there is a uniform velocity profile at the entrance, and null derivatives at the exit. The upper and lower boundary conditions can be chosen either as non-slip to simulate a channel or symmetry for simulating an infinite domain.

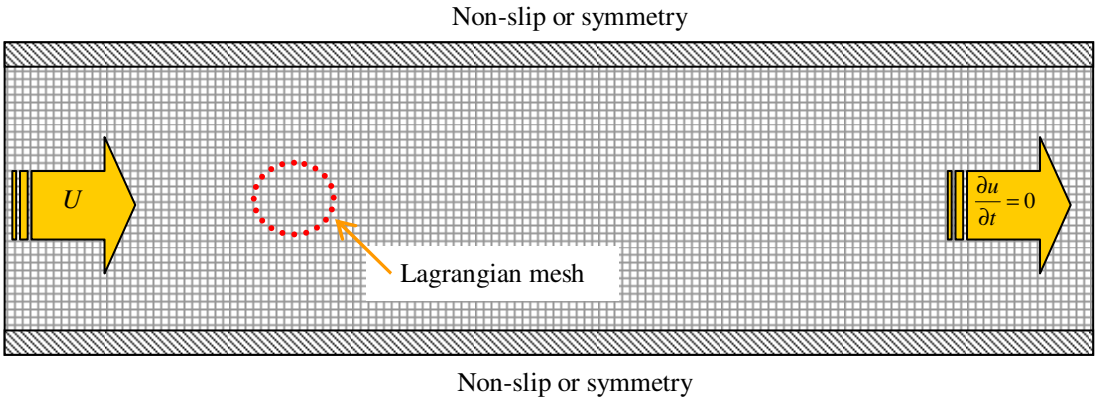

Figure 1: Computational domain and boundary conditions.

4. RESULTS AND DISCUTION

First simulations were of a stationary cylinder in an infinite domain. To search for the lowest computational cost, several meshes were tested and the best configurations are illustrated in Fig. 2, where the Eulerian mesh is uniform only in the neighborhood of the cylinder ($2D$ x $2D$). For the rest of the domain, the mesh is not uniform, and its cells become bigger as they are near the domain boundary. To avoid numerical problems, the mesh expansion rate is limited to 3%.

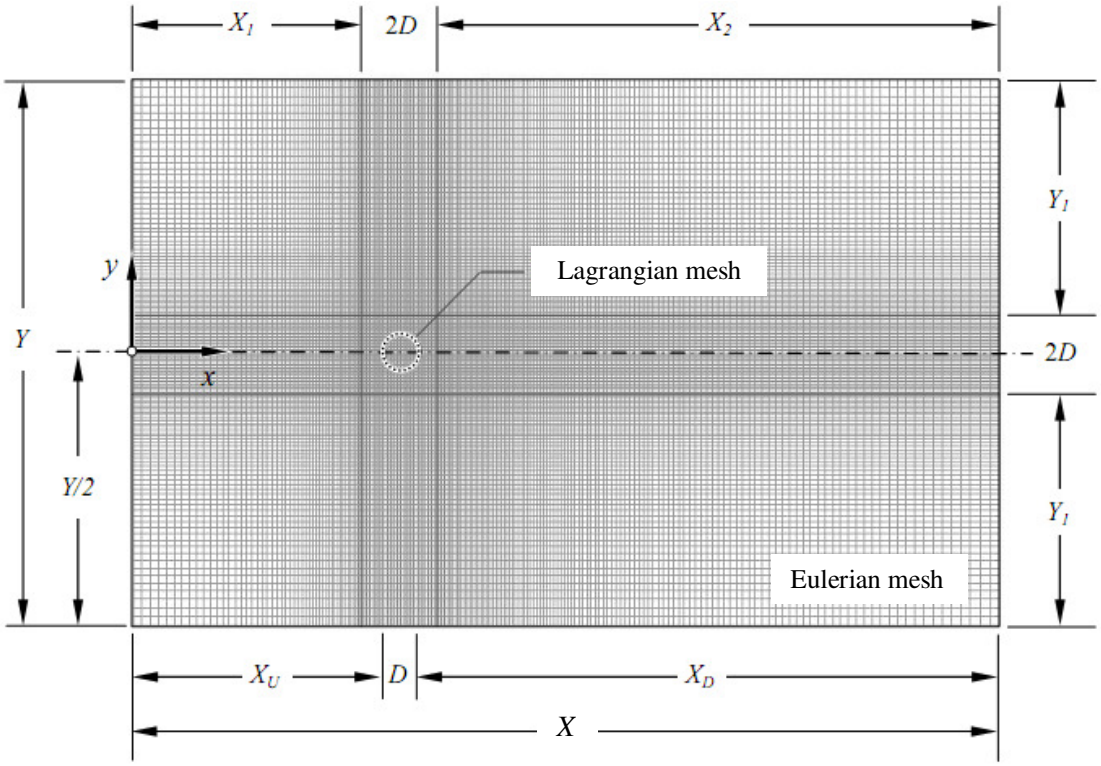

Figure 2: Mesh and computational domain used for stationary non confined cylinder.

According to the literature, the rate between the Lagrangian and the Eulerian meshes must be close to 1.0. A coarse Lagrangian mesh causes a bad representation of the immersed boundaries, while an unnecessary refinement increases the computational costs. Due to this fact, the mesh configuration must be carefully chosen in order to assure physically consistent results, and to save CPU time and memory space. The characteristics of the meshes used in the present simulations are detailed in the Tab. 1.

Table 1: Mesh characteristics.

Mesh	Amount of Lagrangian points	Dimensions			Amount of volumes				Expansion ratio		
		X_U	X_D	Y	X x Y	X_1	X_2	Y_1	X_1	X_2	Y_1
M1	32	7D	16D	15D	135 x 90	35	80	35	3.0%	1.5%	3.0%
M2	64	7D	16D	15D	210 x 144	52	118	52	3.0%	1.5%	3.0%
M3	64	7D	16D	21D	210 x 144	52	118	62	3.0%	1.5%	3.0%
M4	64	10D	16D	21D	215 x 164	62	113	62	3.0%	1.5%	3.0%
M5	64	15D	16D	15D	263 x 144	110	113	52	1.5%	1.5%	3.0%
M6	64	15D	16D	21D	263 x 164	110	113	62	1.5%	1.5%	3.0%
M7	128	7D	16D	15D	308 x 226	73	155	73	3.0%	1.5%	3.0%

For a Reynolds number around 20, the mesh convergence was verified and different schemes were tested for advective terms. The results are presented in Tab. 2. C_D is the drag coefficient, C_L is the lift coefficient, and L_W/D is the ratio between the recirculation bubble length and the cylinder diameter.

Table 2: Non-dimensional parameters for diverse mesh sizes and interpolative schemes.

Mesh	Scheme / Authors	C_D	C_L	L_W/D
M1	CDS	2.83	$1.08\ 10^{-4}$	1.19
	POWER-LAW	2.44	$8.32\ 10^{-6}$	1.19
	QUICK	2.52	$3.88\ 10^{-2}$	1.19
	UDS	2.57	$1.01\ 10^{-4}$	1.19
M2	CDS	2.41	$1.47\ 10^{-4}$	1.05
	POWER-LAW	2.32	$8.78\ 10^{-5}$	1.10
	QUICK	2.38	$2.20\ 10^{-2}$	1.10
	UDS	2.40	$1.44\ 10^{-4}$	1.05
M7	CDS	2.32	$5.11\ 10^{-5}$	1.01
	POWER-LAW	2.28	$2.19\ 10^{-5}$	1.01
	QUICK	2.31	$1.20\ 10^{-2}$	1.01
	UDS	2.32	$5.13\ 10^{-5}$	1.01
	Park *et al.* (1998)	2.01	-	-
	Dennis and Chang (1970)	2.05	-	-
	Su e*t al.* (2007)	2.20	-	-
	Tritton (1959)	2.22	-	-
	Coutanceau and Bouard (1977)	-	-	1.00

For the drag coefficients, the results are about 2.7% and 40.7% higher than those reported by others authors. One can note that for a given interpolation scheme, C_D coefficients results become better with a smaller mesh size. This same behavior can be observed for the recirculation bubble length. Results for the lift coefficients, C_L are near zero, but not null, as they should to be, and the QUICK scheme produced the largest difference when compared to the other schemes.

For a Reynolds number around 200, utilizing CDS, some qualitative results can be visualized in Fig. 3 and quantitatively compared in Tab. 3 with data from other authors. For this case, the calculated Strouhal number is $St = 0.1623$. In Fig. 4 one can note this value is close to the experimental results obtained by Roshko (1954) and Lindquist *et al.* (1999).

As it can be seen in Tab. 3, for moderate Reynolds number of about 200, the lift coefficient results are acceptable. But the values for the drag coefficient are about 40% lower than the smallest founded in the literature. The results deteriorate with an increase in the Reynolds number.

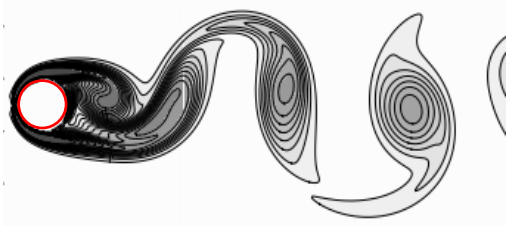

(a) Góis (2007).

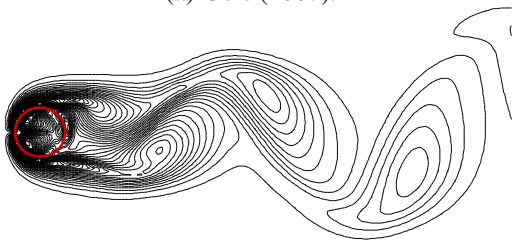

(b) Present work.

Figure 3: Isovorticity contours for a stationary non confined cylinder at Re = 200.

Table 3: Non-dimensional parameters C_D and C_L for Reynolds number around 200.

Authors	C_D	C_L
Liu *et al.* (1998)	1.17 to 1.58	0.5 to 0.69
Góis (2007)	1.39	0.63
Present work	0.49	0.61

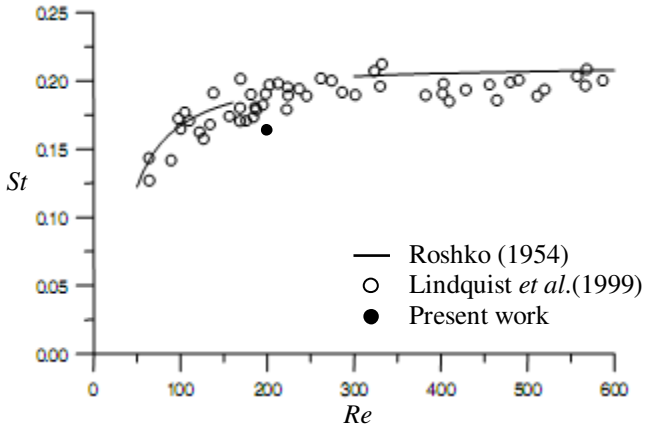

Figure 4: Strouhal x Reynolds relationship for a circular cylinder.

Next simulations consist in the flow around an oscillating cylinder in an infinite domain. The oscillating movement, in the x direction is given by

$$cx = cx_0 + A\,F\cos(t) \tag{9}$$

where cx is the position of the center of the cylinder, cx_0 is the position of the center of the cylinder in the beginning, A is the cylinder oscillation amplitude, and F is the ratio between the cylinder oscillating frequency and the natural vortex shedding frequency.

Figure 5 shows the results for $F = 0.55$ and $A = 0.1$, compared to those of Góis (2007). One can note only a small difference in the lift coefficient values. The maximum for the present work is about 0.7 while for the results of Góis (2007) the maximum is about 0.8. The first seconds of simulation are not shown because the results are not realistic. This happened due to the fact the program evaluates the immersed boundary force only once, and then runs until the next time step. This fact allows the code to run faster, but giving completely unrealistic results during the first seconds.

When dealing with moving boundaries, one important aspect is determining the waiting time before moving the boundary. If the cylinder starts to oscillate in the firsts time steps of the simulation, probably, the program will diverge. It is necessary to wait the first seconds with the immersed boundary stationary, to avoid using physically inconsistent results.

The waiting time and the different implementation of the immersed boundary method used are probably responsible for the small difference in the frequency between both results.

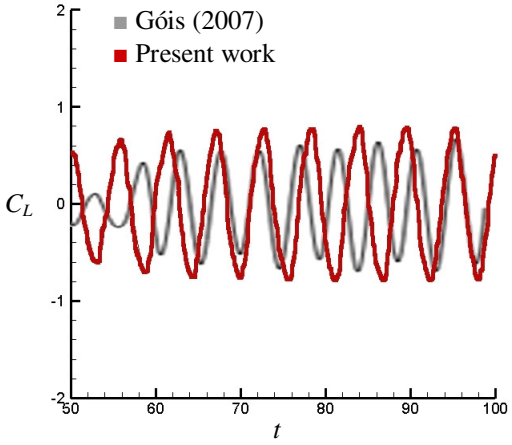

Figure 5: Oscillating cylinder with $A = 0.1$, $F = 0.55$ and $Re = 200$.

Figure 6 shows similar results for $A = 0.1$, $F = 2.2$ and $Re = 200$. The lift coefficients also agree with those in the literature.

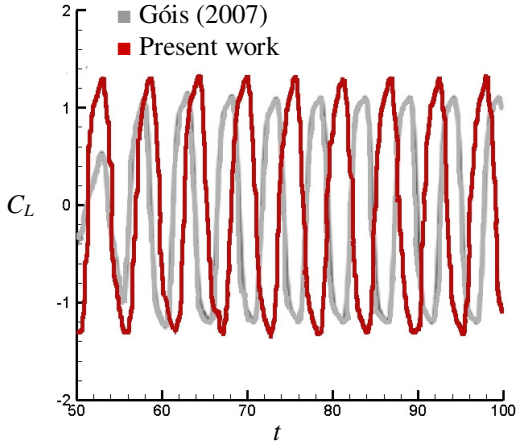

Figure 6: Lift coefficients for $A = 0.1$, $F = 2.2$, and $Re = 200$.

Introducing a tangential velocity in the Lagrangian points, a rotational movement is given to the cylinder. Tests were made for $Re = 60$ and several specific accelerations ranging $0 \leq \alpha \leq 1.8$. For this case, even thought the flow is still laminar, the lilt and drag coefficients are alternated due to the periodic vortex shedding. The simulations used the mesh M6 and the Power-Law for advective terms treatment. Figure 7 shows results for stream lines and pressure fields for a stationary cylinder ($\alpha = 0$) and a rotational cylinder ($\alpha = 1.4$). The moving cylinder presents deformed and non symmetric stream lines outside the cylinder, and inside the cylinder, the flow starts to rotate like a rigid body. For a stationary cylinder, the highest pressures were located at the stagnation point, however, for a rotational cylinder, the high pressures move to the bottom for the cylinder with counterclockwise rotation, generating an additional lift force.

Using the non-slip conditions, the flow inside a channel can be simulated and the blockage effects in the flow past the cylinder can be verified.

The fluid flow inside a channel is governed by the Reynolds number and the blockage ratio, here defined as $\lambda = H/D$, where H is the distance between the walls and D the diameter of the cylinder. Figure 8 shows a diagram for vorticity, stream lines and the length of the recirculation bubble L_W (in meters) versus time t (in seconds), in a channel with $\lambda = 1.9$ and $Re = 54$. The flow becomes unsteady after 50 s of simulation. Comparing the present results with those

found in the literature, the unconfined flow over a cylinder, for $Re = 54$, presents periodic vortex shedding, while with a blockage ratio $\lambda = 1.9$, the flow becomes unsteady. According to the results of Chakraborty (2004), the force applied to the flow by the walls, is responsible for the enlargement of the bubble and a delay in the vortex shedding.

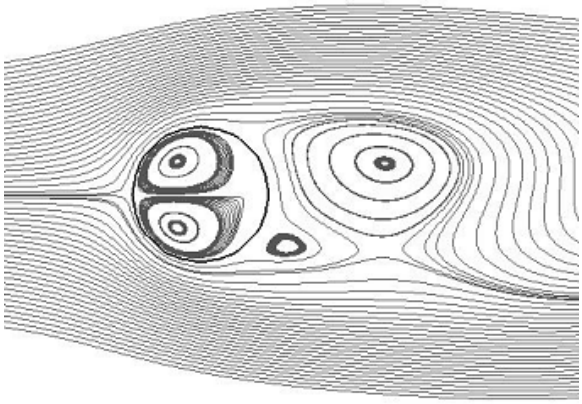

(a) Stream lines, $\alpha = 0$.

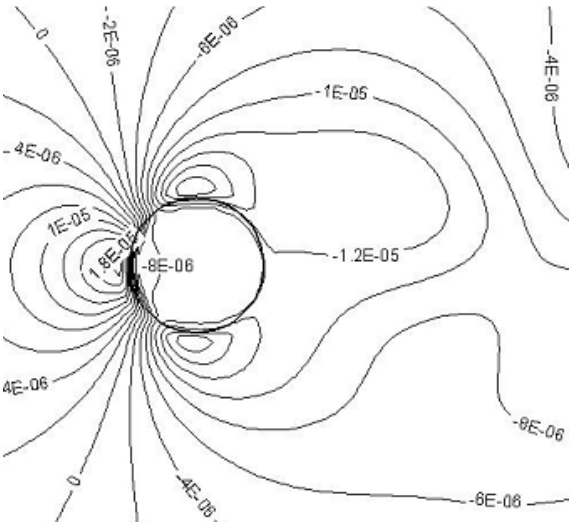

(b) Pressure fields, $\alpha = 0$.

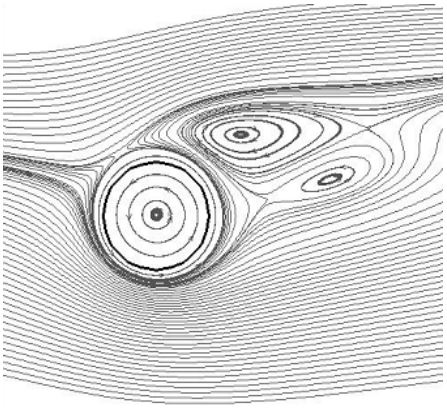

(c) Stream lines, $\alpha = 1.4$.

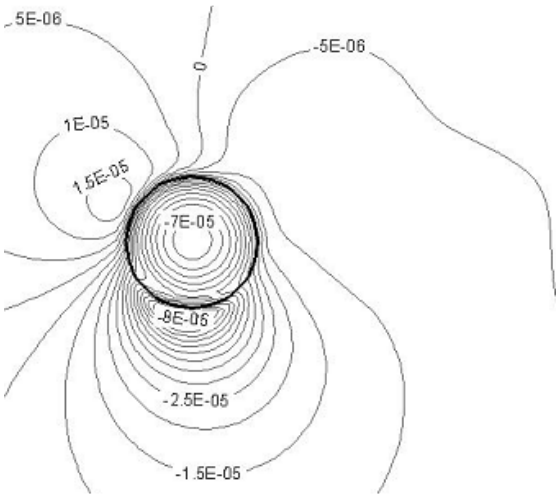

(d) Pressure fields, $\alpha = 1.4$.

Figure 7: Rotational cylinder comparing results.

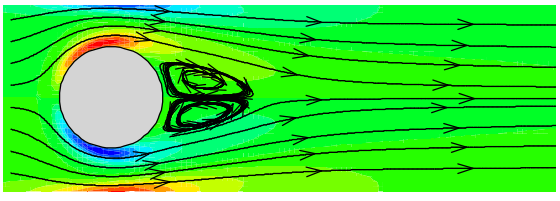

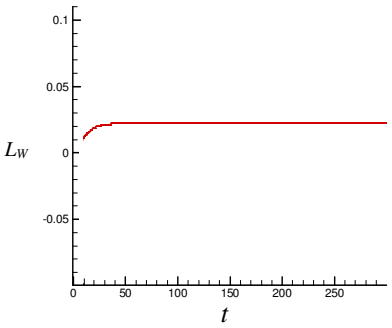

Figure 8: Flow around a confined cylinder with $\lambda = 1.9$ and $Re = 54$.

Increasing the Reynolds number to $Re = 100$ and keeping the same blockage ratio $\lambda = 1.9$, Fig. 9 shows the flow time evolution. The flow remains steady until $t = 320$, when the two halves of the bubble start to increase their sizes and eventually splitting, resulting in periodic vortex shedding.

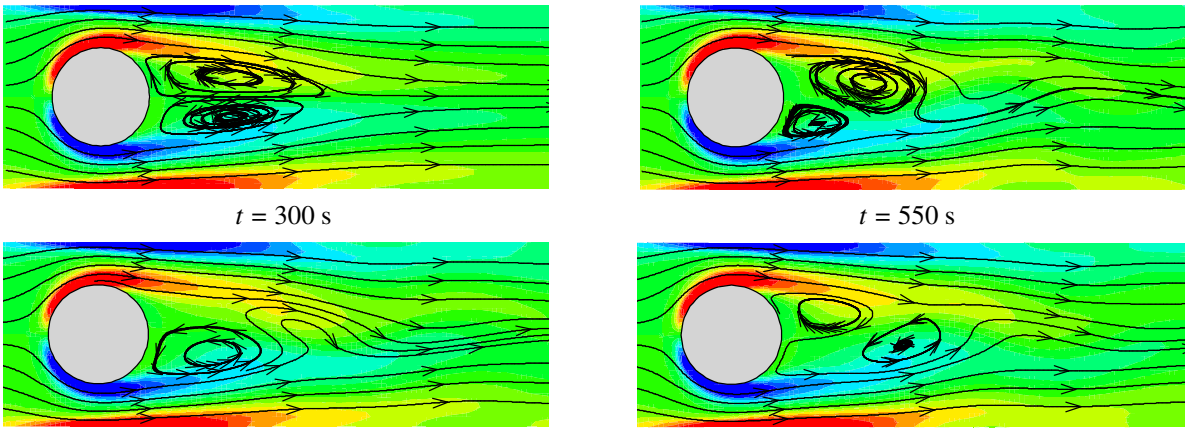

Figure 9: Flow around a confined cylinder with $\lambda = 1.9$ and $Re = 100$.

With a further increase in the Reynolds number, $Re = 200$, the periodic vortex shedding starts early at about $t = 70$ s, as can be seen in Fig. 10. A non confined cylinder, for a $Re = 200$, presents a maximum lift coefficient of 0.61, as seen in Tab. 3. The diameter of the vortex is bigger for non confined cylinders. The drag coefficient increases due to the walls and the lift coefficient remains almost the same, in agreement with the literature.

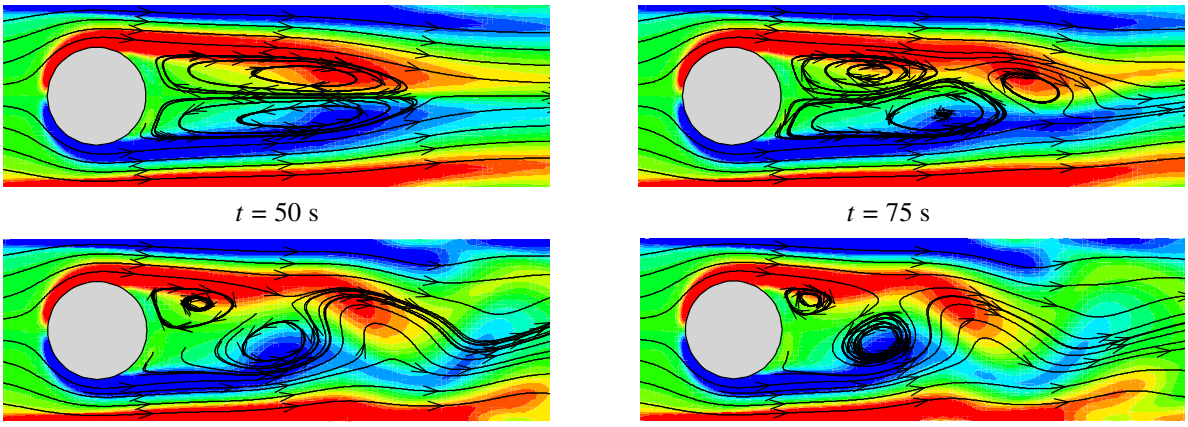

Figure 10: Flow around a confined cylinder with $\lambda = 1.9$ and $Re = 200$.

3. CONCLUSION

The present work is the first step in a long process of improving the Physical Virtual Model which will eventually make it suitable for simulating more complex and moving geometries. Many modifications still are still needed in order to give more accurate results. The low order discretization may be responsible for some of the discrepancies with the literature, and in some special cases, the appearance of numerical instabilities. One important next step would be the code parallelization and the use of other methods like the factional steps method.

4. ACKNOWLEDGEMENTS

The authors are grateful to FAPESP, CAPES and FUNDUNESP for providing the financial support which made this work possible. The first author also wishes to thank Foreign Affairs and International Trade Canada for sponsoring her stay in Canada through the Graduate Students' Exchange Program (GSEP).

5. REFERENCES

Balaras, E., 2004, “Modeling complex boundaries using an external force field on fixed Cartesian grids in large-eddy simulations”. Comput. Fluids, Vol.33, pp.375-404.

Bornschlegell, A.B., 2008, "Implementação e Teste do Método da Fronteira Imersa para a Simulação do Escoamento em Torno de Cilindros Estacionários e Rotativos", M.Sc. Dissertation, São Paulo State University – UNESP, Ilha Solteira, SP, Brazil, 75 p.

Campregher, R.J., 2002, "Simulação Numérica de Escoamentos Transicionais e Turbulentos ao Redor de Geometrias Cartesianas", M.Sc. Dissertation, São Paulo State University – UNESP, Ilha Solteira, SP, Brazil, 135 p.

Chakraborty, J., Verma, N., Chhabra, R.P., 2004, "Wall effecting flow past a circular cylinder in a plane channel: a numerical study", Chem. Eng. Proc., Vol.43, Issue 12.

Fauci, L.J., McDonald, A., 1994, "Sperm motility in the presence of boundaries", Bull. Math. Biol. Vol.57, pp.679-699.

Lima e Silva, A.L.F., 2002, "Desenvolvimento e Implementação de uma Nova Metodologia para Modelagem de Escoamento sobre Geometrias Complexas: Método da Fronteira Imersa com Modelo Físico Virtual", Ph.D. Thesis, University of Uberlândia – UFU, Uberlândia, Brazil, 138 p.

Lindquist, C., Vieira, E.D.R, Mansur, S.S, 1999, "Flow visualization of the von Kármán vortex street: a tool for fluid mechanics learning", Proc. of the Int. Congress on Eng. and Compt. Education – ICECE'99, Rio de Janeiro, pp.1-4.

Mittal, R., Iaccarino, G., 2005, "Immersed boundary methods", Annu. Rev. Fluid Mech., pp.239-261.

Peskin, C.S., 1977, "Numerical analysis of blood flow in the heart", J. Comput. Phys., Vol.25, pp.220-252.

Roshko, A., 1954, "On the Development of Turbulent Wakes from Vortex Streets", NACA Reporter 1191.

Verzicco, R., Mohd-Yusof, J., Orlandi, P., Haworth, D., 2000, "LES in complex geometries using boundary body forces", AIAA Journal, Vol.38, pp.427-433.

6. RESPONSIBILITY NOTICE

The authors are the only responsible for the printed material included in this paper.